© 2017. Published by The Company of Biologists Ltd | Journal of Experimental Biology (2017) 220, 3771-3781 doi:10.1242/jeb.166413

RESEARCH ARTICLE

Novel neurobiological properties of elements in the escape circuitry of the shrimp

De Forest Mellon, Jr

ABSTRACT

Escape behaviors in penaeid shrimp are mediated by large myelinated medial giant fibers which course from the brain to the last abdominal ganglion in the ventral nerve cord. In each abdominal segment, the medial giant axons make synaptic connections with paired myelinated motor giant axons that excite the abdominal deep flexor muscles and drive the tailflips that constitute the escape behavior. I examined (1) anatomical features of the abdominal motor giant fibers and (2) electrical properties of both the medial and motor giant axons in the pink shrimp, *Farfantepenaeus duorarum*. The motor giant axons in the paired third roots of shrimp abdominal ganglia emerge from a single fused neurite that originates from two clusters of cell bodies within the ganglion. Injection of large positive currents into the abdominal medial giant fibers generates action potentials that are transmitted to the opposite medial giant axon through putative collateral synapses within the ganglia. Transmission across the medial-to-motor giant synapse is fast and resistant to fatigue, with synaptic delays equal to or less than those previously documented at the lateral-to-motor giant electrical synapse in crayfish. Transmission was found to be extremely reliable even with presynaptic spike frequencies as high as 250 Hz. While action potentials within the medial giant fibers are transmitted across the medial-to-motor giant synapse with a large safety factor, neither prolonged positive nor prolonged negative currents pass through the synaptic nexus, irrespective of the site of injection. The lack of DC current passage along with the inability of neurobiotin or biocytin to spread through the synaptic nexus raises the possibility that the synaptic mechanism may be capacitative.

KEY WORDS: Escape response, Giant fibers, Synapse

INTRODUCTION

Escape reflexes are characteristic behaviors exhibited by most macruran decapod crustaceans, such as shrimp, crayfish and lobsters, to avoid predation. During these behaviors, referred to as tailflips, the abdominal segments are rapidly and massively flexed and drive the animal rearward through the water column away from potential sources of danger. Tailflips are triggered by both visual and hydrodynamic inputs (Wine and Krasne, 1982; Mellon and Christensen-Lagay, 2008; Liu and Herberholz, 2010), and they rely upon rapid synaptic transmission between afferent systems and dedicated giant interneurons, rapid conduction velocities in those interneurons and rapid synaptic transfer to giant motor neurons that directly activate the abdominal flexor muscles. In crayfish, for example, the latency of the motor response underlying these reflexes following appropriate sensory stimulation can be as short as 8 ms (Krasne and Wine, 1975).

Escape reflexes in shrimp and prawns are also mediated by giant interneurons. The medial giant axons in both of these groups are myelinated, promoting extremely high action potential (AP) conduction; the conduction velocity of APs in medial giant fibers of penaeid shrimp is the highest recorded in any animal system, up to 220 m s^{-1} at 18°C (Fan et al., 1961; Kusano, 1966; Kusano and LaVail, 1971). By comparison, the highest conduction velocities in mammalian systems approach 120 m s^{-1}. Among the factors in shrimp responsible for such rapid propagation include saltatory impulse conduction analogous to that found in myelinated vertebrate nerve fibers (Hsu and Terakawa, 1996) and extremely rapid voltage-gated sodium channel kinetics (Terakawa and Hsu, 1991).

Within the abdominal nerve cord of penaeids, functional nodes occur in the myelin sheath of the medial giant fibers at each ganglion, as well as periodically along the interganglionic connectives. Kusano and LaVail (1971) used an extracellular electrode to measure inward current sinks along the abdominal ventral nerve cord (VNC) of *Penaeus japonicas*. They reported the presence of current sinks (nodes) at each abdominal ganglion and in the region of the medial-to-motor giant fiber synapse, where the third roots emerge from the VNC. Later studies by Hsu and Terakawa (1999), using the shrimp *Penaeus chinensis*, suggested the presence of additional nodes approximately every 10 mm along the interganglionic segments of the medial giant fibers. Within the ganglia, unmyelinated small branches of the medial giant axons serve as functional nodes. In the interganglionic regions of the axons, however, nodes are specialized structures, termed fenestration nodes (Hsu and Terakawa, 1996, 1999), consisting of small (<50 µm) oval windows in the myelin sheath that expose the axonal membrane directly to the extracellular space. The voltage-gated sodium and potassium channels that are the basis for the propagated APs (Terakawa and Hsu, 1991) presumably are specifically confined to the nodal areas of the axonal membrane.

Of considerable interest is transmission between the medial giant axons and the myelinated motor giant axons that drive the flexor musculature in each abdominal segment. In the crayfish, analogous synaptic transmission between the lateral giant axons and the abdominal motor giant axons was found to be electrical and voltage dependent, with current passing directly into the motor giant axons from APs in the lateral giant axon (Furshpan and Potter, 1959). Current from antidromic APs evoked in motor giant axons does not pass across the synapse into the lateral giant axon because of the rectifying voltage dependence of the synapse. Orthodromic transmission across this electrical synapse is fast, with a delay of only about 120 µs at 20°C. The rapidity of synaptic transfer between the medial giant axons and the motor giant axons in shrimp has not previously been studied, but it must also be very high.

In penaeid shrimp, the anatomy of the motor giant neurons in the abdominal segments is more complex than that found in crayfish.

University of Virginia, Department of Biology, 485 McCormick Road, Charlottesville, VA 22903, USA.

*Author for correspondence (dm6d@eservices.virginia.edu)

De F.M., 0000-0002-5701-7909

Received 10 July 2017; Accepted 15 August 2017

Journal of Experimental Biology (2017) 220, 3771-3781 doi:10.1242/jeb.166413

The motor giant axons arise from paired clusters of approximately 30–40 somata in each abdominal ganglion (De F.M., unpublished observations), and their respective neurites, as in prawns (Johnson, 1924; Holmes, 1942), fuse with one another and also with their contralateral counterparts to form a single, myelin-clad neurite that courses caudally toward the paired third roots (Kusano, 1966; Faulkes, 2015; De F.M., unpublished observations). Rostral to the exit point of the third roots in each ganglion, the fused motor giant neurite bifurcates to two separate axons that exit the third root. Just caudal to the point of bifurcation of the motor giant neurite, its two branches pass ventral to their ipsilateral medial giant axon and are synaptically connected to it (Kusano, 1966; Kusano and LaVail, 1971). In the vicinity of the medial-to-motor giant synapse, the membrane of the presynaptic (medial) giant fiber exhibits a functional node (Kusano and LaVail, 1971), identified by Terakawa and Hsu (1991) as a fenestration node. At this point, the giant fiber's myelin sheath is interrupted; however, the anatomical relationship of this nodal structure with respect to the synaptic membrane is not clear. Electronmicroscopical study of the medial-to-motor giant synapse (Kusano and LaVail, 1971), indicated that both presynaptic and postsynaptic axons lose their myelin and surrounding Schwann cell sheaths in the immediate region of this synaptic contact. The axons make gap junction-like direct contacts with one another, suggesting that the synapse functions by direct electrical transfer, as in crayfish (Robertson, 1955; Furshpan and Potter, 1959). One possible anatomical arrangement would be for the synaptic contact to be surrounded by the axonal membranes of the adjacent fenestration nodes in the medial giant and the motor giant axon.

I undertook an electrophysiological examination of the medial giant fiber–motor giant fiber synaptic relationships in the pink shrimp *Farfantepenaeus duorarum* by simultaneous electrical recordings from both medial giant fibers and from the fused motor giant axon in the same abdominal segment. The results indicate that synaptic transfer is very fast, occurring in less than 90 µs in most instances at 17.5°C and is assumed, therefore, to be electrical. My findings also suggest that maximally effective transfer of excitation occurs when APs in both medial giant axons arrive at their respective synaptic loci simultaneously. This must normally occur, as the two medial giants appear to be interconnected, apparently through functional relationships within the abdominal ganglia (see below), but possibly also within the brain where their cell bodies reside (Kusano, 1966). Synaptic transfer is robust, in one case being maintained without temporal jitter for more than 300 cycles at 250 Hz. Curiously, direct passage of current in either direction across the medial-to-motor giant synapse does not occur. This suggests the hypothesis that synaptic transfer may be ephaptic in nature.

MATERIALS AND METHODS

Pink shrimp *F. duorarum* (Burkenroad 1939), 10–15 cm long, of both sexes, were obtained from Gulf Specimen Marine Laboratories (Panacea, FL, USA) and maintained in artificial seawater at room temperature until used. Prior to dissection, an animal was placed on crushed ice for 5–15 min to anesthetize it, following which the cephalothorax was separated from the abdomen using sharp scissors. The abdomen was pinned out ventral side up to the Sylgard floor of a dissecting dish and immersed in chilled shrimp saline having the following composition: NaCl, 455 mmol l^{-1}; KCl, 10 mmol l^{-1}; $CaCl_2{\cdot}2H_2O$, 23 mmol l^{-1}; $MgCl_2{\cdot}7H_2O$, 13 mmol l^{-1}; $NaHCO_3$, 2 mmol l^{-1}. The pH of the saline was adjusted to 7.4 prior to use with HCl or NaOH.

Anatomical procedures

Motor giant axons were filled with a 2% mixture of biocytin (Sigma-Aldrich, St Louis, MO, USA) and neurobiotin (Vector Laboratories, Burlingame, CA, USA) dissolved in deionized water. The abdomen of a shrimp was pinned down ventral side up in a saline-filled dissection chamber. The swimmerets were removed and an abdominal ganglion was exposed by dissecting away the overlying cuticle. The third roots in the ganglion were located, and the giant motor fibers, still attached to their target musculature, were visualized where they emerged from the VNC. The tips of sharp micropipette electrodes, having resistances of 15–20 MΩ, were filled with the biocytin/neurobiotin mixture and the electrode shank was then filled with 200 mmol l^{-1} KCl. The microelectrode was then inserted into an electrode holder and connected to the input stage of an Axoclamp 2B electrophysiological amplifier (Molecular Devices, Sunnyvale, CA, USA). A micromanipulator was used to drive the electrode tip through the myelin sheath of the motor giant fiber and into the axon within the third root. Axonal penetrations were assumed when the electrical potential recorded by the electrode measured a steady −75 to −80 mV. At that point, rectangular pulses of 2–3 nA of positive current were passed into the axon at 1 Hz with a 50% duty cycle. Axons were filled with the biocytin/neurobiotin mixture for 1–2 h at approximately room temperature, following which that section of the VNC containing the ganglion under examination was removed to a vial of 4% paraformaldehyde made up in 0.1 mol l^{-1} sodium phosphate buffer, adjusted to a pH 7.4. The ganglion was fixed overnight at 4°C, washed in several changes of plain phosphate buffer for 15 min each, and transferred to a vial with 0.3% Triton-X 100 made up in phosphate-buffered saline for 1 h. The tissue was then incubated in a 1:150 dilution of streptavidin tagged with Alexafluor 488 in 0.3% Triton-X phosphate-buffered saline for 24–36 h at 4°C on a rocking table. Suitably stained ganglia were rinsed in phosphate-buffered saline, dehydrated in an ethanol series, cleared in methyl salicylate, and photographed as whole mounts with a digital camera mounted on an epifluorescence binocular microscope.

Cobalt-stained preparations were prepared in the following manner. An abdominal ganglion with its third roots was dissected free of the VNC and pinned out in a small Sylgard-lined dish in shrimp saline. Vaseline wells were constructed to surround the severed ends of the third roots; the saline within the wells was then exchanged for a solution of 0.3 mol l^{-1} cobalt chloride made up in deionized water. The preparation dish was then covered and incubated at 4°C for 24–48 h, after which it was placed in fresh shrimp saline to which 1–3 drops of ammonium sulfide was added. In those preparations that had been successfully backfilled with cobalt, the black precipitated cobalt sulfide especially filled the motor giant axons and cell bodies. These preparations were dehydrated through an ethanol series, cleared in methyl salicylate, and photographed as whole mounts.

Physiological procedures

Shrimp were placed on crushed ice for 15 min to anesthetize them. The abdomen was severed from the cephalothorax, mounted ventral side up in a Sylgard-lined dissection dish and covered with chilled saline. The swimmerets were excised from the abdominal segments and a longitudinal midline cut was made in the ventral cuticle from the last thoracic ganglion to the fifth abdominal ganglion. The exposed VNC was ligated with fine nylon thread at the last thoracic ganglion and caudal to the fourth abdominal ganglion, following which all abdominal ganglionic nerve roots were transected, with the exception of the paired third roots in the first or second

Journal of Experimental Biology

Journal of Experimental Biology (2017) 220, 3771-3781 doi:10.1242/jeb.166413

abdominal ganglion. These roots were severed as far laterally as possible; additionally, smaller dorsal branches of the motor giant fibers were also severed. The isolated VNC was then transferred to a recording chamber and immersed in fresh, chilled shrimp saline. Using stainless steel minuten nadeln, the VNC was pinned to the Sylgard floor of the chamber, dorsal side up, by pins at the rostral and caudal ends of the VNC. Additional pairs of minute pins through the lateral portions of the first and second or the second and third abdominal ganglia stabilized the section of the VNC between the second ganglion and the point of emergence of its severed third roots. This portion of the VNC was then cleaned of the attached dorsal artery, and the connective tissue sheath overlying the paired medial giant fibers was carefully stripped away. The fused motor giant axon, lying directly beneath the narrow space between the two medial giant fibers, was usually visible at this point (see Fig. 2 and Kusano, 1966). Electrical stimulation of the VNC was accomplished by transecting the cord just caudal to the last thoracic ganglion or just rostral to the fifth abdominal ganglion and pulling the section of the VNC either between the last thoracic and first abdominal ganglion or between the fourth and fifth abdominal ganglia into a suction stimulating electrode. Electrical pulses of 0.01–0.02 ms duration were delivered at a frequency of 1 Hz to the cord via a Grass S88 stimulator and isolation unit (Natus Neurology-Grass, Warwick, RI, USA). Three glass micropipette electrodes filled with 3 mol l^{-1} KCl and having resistances of 15–20 MΩ were used to simultaneously record electrical activity from the two medial giant fibers and the motor giant fiber, and/or to pass current into the axons or into the gap between the axons and their myelin sheaths. Although penetration of the fused motor giant fiber usually resulted in intracellular recording from the axon itself, medial giant fiber recordings were usually obtained from the gap region between the myelin sheath and the much smaller diameter axon. Care was taken to penetrate the motor giant fiber near the bifurcation region (near the presumed site of synaptic transfer); penetration of the medial giant fibers occurred at approximately the same position along the VNC, usually slightly more rostral than the motor giant fiber electrode. In a few preparations, motor giant fiber recordings were obtained from the third roots in minimally dissected preparations, because transection of the motor giant fiber branches appeared to affect the electrical characteristics of the synaptic connection.

Electrical activity was fed via electrode holders to the input probes of either an Axoclamp 2B dual channel amplifier (Molecular Devices), operated in bridge mode, or a Getting microelectrode single channel preamplifier (no longer commercially available). One channel (V2) of the Axoclamp 2B was used to deliver the large currents required to excite the medial giant fibers via the microelectrodes. Signals were simultaneously led to an analog oscilloscope and a digitizer (Axon Instruments Digidata 13A, Molecular Devices), then to a computer running data acquisition software (pCLAMP 8.2) for later analysis.

Recording from and directly stimulating the medial giant axons were usually accomplished from the gap region of the fibers, between the myelin sheath and the axons themselves. While the medial giant fibers themselves are up to 150 µm in diameter, their enclosed axons have a diameter of little more than 10 µm (Kusano, 1966). The extremely high electrical resistance of the myelin relative to that of the axonal plasma membrane ensured that action potentials generated at the fenestration nodes had amplitudes in the gap of up to 90 mV; during current injection into the gap, a sizeable fraction of the injected current must have passed through the axonal membrane and excited it at the nearest fenestration node, generating

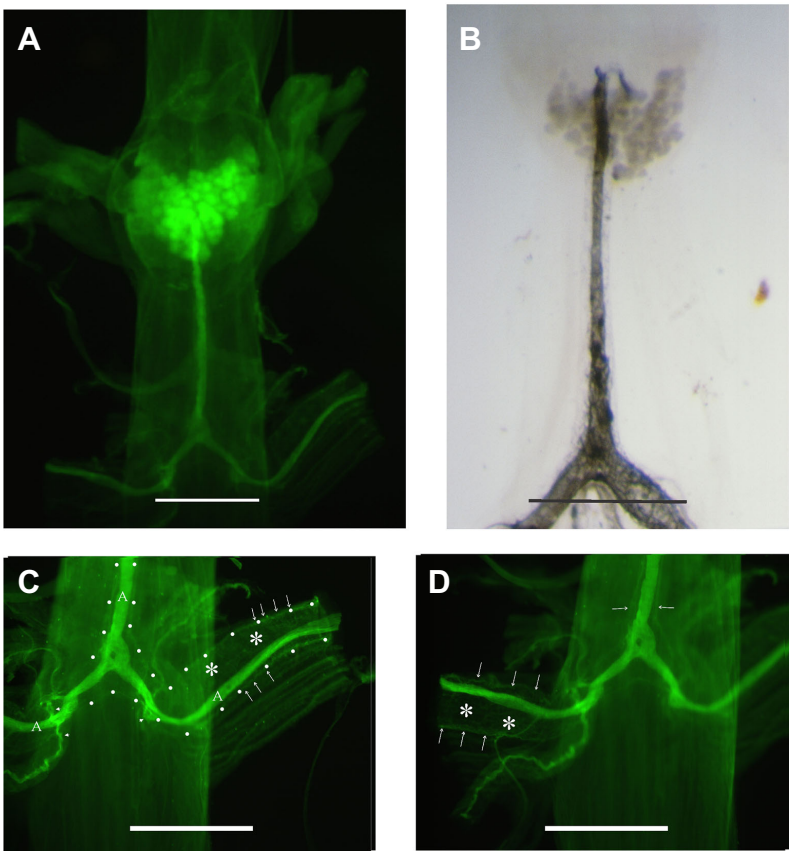

Fig. 1. Labeled shrimp motor giant axons. (A) Dorsal view of a fluorescently labeled motor giant fiber complex in the third abdominal ganglion of the shrimp *Farfantopenaeus duorarum*. The giant motor axons from both sides enter the ventral nerve cord (VNC) via the third ganglionic roots and fuse at the midline, then course rostrally, bifurcate, and terminate in paired clusters of 30–40 cell bodies. Scale bar: 500 µm. (B) Motor giant fiber in an abdominal ganglion of *F. duorarum* that was backfilled with cobalt chloride. Fusion of the two motor giant axons at the midline is evident; rostrally, the fused axon/neurite bifurcates to terminate in paired bilateral clusters of cell bodies. Scale bar: 500 µm. (C) Ventral view of the motor giant complex, imaged at higher magnification. The myelin sheath enclosing the left giant motor axon is indicated by both white arrows and white dots. The submyelinic gap between the axon and the myelin sheath is indicated by white asterisks. The fluorescently labeled axons are indicated by the letter A. Several smaller branches from the motor giant axons are visible (arrowheads). (D) Ventral view of the right motor axon branch, the myelin sheath enclosing it and the fused central portion indicated by white arrows. Asterisks as in C. Scale bars: 500 µm.

Journal of Experimental Biology (2017) 220, 3771-3781 doi:10.1242/jeb.166413

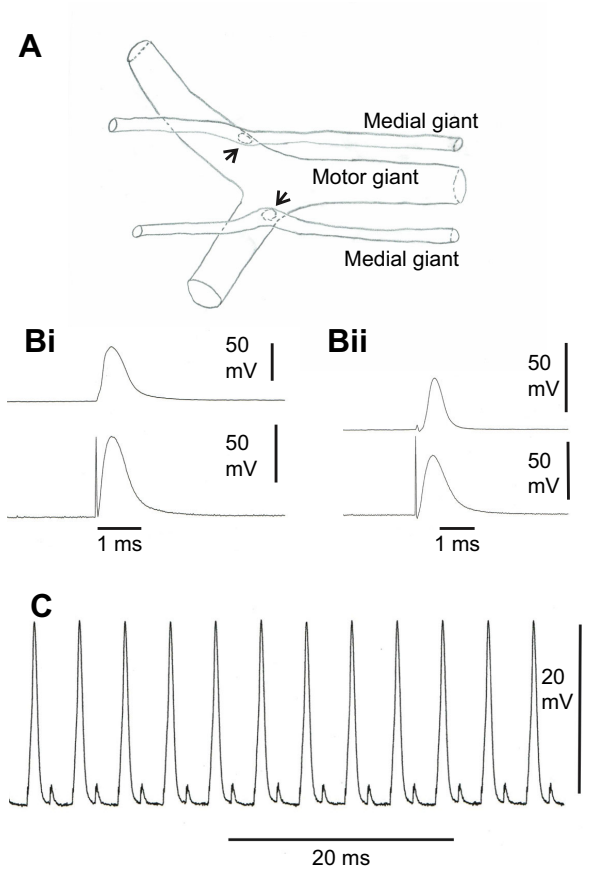

Fig. 2. Anatomical and electrical relationships of the medial-to-motor giant synapse. (A) Simplified diagram of the anatomical relationship between the medial giant axons and the motor giant axon at the exit point of the third ganglionic roots. Just rostral to the emergence of the third roots, the medial giant fibers cross dorsally to the bifurcated motor giant branches, at which point the medial giant fibers synapse with the motor giant fibers (arrows). (B) Simultaneous electrical recordings from medial and motor giant fibers in the second abdominal segment of the VNC of *F. duorarum*. Bi shows recordings from the submyelinic gap in a medial giant (lower trace) and motor giant (upper trace) fiber following generation of an action potential (AP) at the rostral end of the abdominal nerve cord. Bii shows similar records from another preparation in which the motor giant electrode (upper trace) was intra-axonal. (C) Part of a postsynaptic AP train in a motor giant fiber in response to electrical stimulation of the VNC at nearly 500 Hz. The postsynaptic spikes exhibited no apparent temporal jitter or amplitude diminution for at least 335 cycles.

an AP. Positive currents of 90–200 nA were necessary to accomplish this mode of AP generation. Recording from and stimulating the motor giant fiber was usually done from intracellular electrodes within the axon itself, as, between the third roots and the ganglion, the fused motor axon is nearly the same diameter as that of the myelin sheath. Intra-axonal penetration was confirmed by a resting potential of −60 to −75 mV. All electrophysiological experiments were performed in shrimp saline at a controlled bath temperature of 17.5°C.

RESULTS

Motor giant neuron anatomy

Fig. 1A is a dorsal view of the fluorescently labeled motor giant fiber within the second abdominal ganglion of *F. duorarum*. Individual myelin-enclosed giant motor axonal branches from the paired third roots fuse at the midline just rostral to their exit point from the VNC. Within the fused section of the motor giant, the axon itself is relatively wide compared with its myelin sheath; as it emerges on each side from the VNC, however, its myelin sheath increases in diameter to exceed that of the axon (Fig. 1B). This creates a large submyelinic gap between the axon itself and its surrounding myelin sheath, as is also the case for the medial giant fibers. Within the ganglion, the individual neurites from two clusters of ventrally located cell bodies [identified by Faulkes (2015) as a single pair of giant irregularly shaped somata] fuse to generate the large central neurite of the motor giant fiber. There was no indication that the biocytin/neurobiotin mixture migrated across the synaptic contacts with the medial giant axons, as the latter were never labeled following injection of the dye into the motor giant axon. The same complex of features can be seen in a cobalt chloride-filled motor giant in Fig. 1B. In Fig. 1C,D, which shows higher magnification fluorescence images (but at a slightly more ventral focal plane) of the region where the left and right paired axons fuse with one another, outlines of the myelin sheaths are visible (arrows). Careful examination of this and similar images suggests that the paired myelin sheaths from the two branches also fuse into a single tube-like structure rostral to the third roots. The diagram in Fig. 2A, constructed from descriptions in the histological and electron microscopic studies of Kusano (1966) and Kusano and LaVail (1971), suggests the approximate location of the synaptic connection between the medial giant axons and the two major branches of the motor giant axon. Extracellular recordings (Kusano and LaVail, 1971) just rostral to this region, in the fused neurite, suggest the presence of functional nodes in each branch. A voltage-clamp examination of the node currents in the immediate vicinity of the medial-to-motor giant synapse (Terakawa and Hsu, 1991) implied that the synaptic connection and the fenestration node were adjacent to one another, although no detailed anatomical evidence for this was provided.

Electrophysiological findings

Measurement of synaptic delay and evidence for periodic nodes and functional interconnections in the abdominal VNC

I recorded simultaneously from the fused motor giant neurite and one or both of the medial giant axons in the second abdominal segment following AP generation by electrical stimulation. As far as possible, all electrode tips were positioned at the same distance from the motor giant bifurcation rostral to the third roots. In almost all preparations, suprathreshold stimuli to the VNC generated an AP in both medial giant fibers and, with vanishingly small delay, an AP or a subthreshold potential in the motor giant fiber. Fig. 2B,C shows typical examples from two preparations. In Fig. 2B, both the medial giant (lower trace) and the motor giant (upper trace) recording electrodes were in the submyelinic gap. In Fig. 2C, the medial giant recording electrode was in the gap, but the motor giant recording electrode was intracellular and exhibited a resting potential of −61 mV. Fig. 2C illustrates a portion of a postsynaptic response train in a motor giant fiber to repetitive electrical stimuli delivered to the VNC and recurring at about 500 Hz. The postsynaptic AP responded to every other stimulus with an apparent invariant peak separation. I measured spike peak interval in 25 contiguous responses at the beginning of the response train, within the middle of the response train and at the termination of the response train. In each set of 25 measurements, the mean (±s.d.) spike peak interval was found to be 4.05±0.012 ms. The small (40 µs) variations in spike interval were due to measurement errors.

Additional experimental observations of synaptic transfer were performed by recording simultaneously from both medial giant fibers as well as the motor giant. Near-simultaneous action

Journal of Experimental Biology (2017) 220, 3771-3781 doi:10.1242/jeb.166413

potentials evoked electrically in the two medial giant fibers were usually followed by a subthreshold or suprathreshold potential in the fused motor giant fiber recorded between the third roots and the ganglion. Fig. 3A indicates responses from both medial giant fibers and the motor giant fiber simultaneously recorded in the second abdominal segment. The approximate relative positions of the three recording electrodes are shown in Fig. 3B. It is inherently difficult to measure synaptic delay even when the recording electrodes are positioned near the synaptic contact; there is always a measure of uncertainty concerning the timing of the actual start of the AP rising phase. Although the timing of the peaks of the APs can be directly compared, to be meaningful, such a measurement would assume that the rate of rise of the medial giant AP and the motor giant AP are identical, and this has not been shown. Another problem is the possibility that the excitation of the individual medial giant fibers may have occurred at different nodes – that is, at different levels of the VNC – or there could be small differences in conduction velocity in the two axons, complicating assumptions about spike latencies. One or both of these possibilities may have occurred in the records of Fig. 3A; the spike in the left medial giant fiber (Fig. 3Ai) begins and peaks after that of the motor giant fiber (Fig. 3Aii), which presumably was excited previously by the AP in the right medial giant fiber. In their study of the lateral-to-motor giant synaptic delay in the crayfish, Furshpan and Potter (1959) chose to measure the point at which the extrapolated steepest slope on the AP rising phase in the lateral giant fiber crossed the baseline and to compare that with the time at which the steepest slope on the motor giant AP also crossed the baseline. Their results suggested ca. 120 µs for a synaptic delay. Using this technique with the records in Fig. 3A, the synaptic transfer between the right medial giant and the motor giant fiber is rapid and is probably less than 90 µs.

The periodic nodal arrangement in the penaeid abdominal VNC reported previously (Kusano and LaVail, 1971; Hsu and Terakawa, 1996) is supported by my electrophysiological experimental evidence. Fig. 4A,B shows APs in both medial giant fibers recorded rostral to the third roots of the second abdominal ganglion, and generated by brief (0.01 ms) suprathreshold electrical shocks to the VNC just caudal to the fourth abdominal ganglion (black traces). A reduction in the initial shock intensity resulted in a distinct stepwise (i.e. not continuous) increase in the latency of both medial giant APs (blue traces). These and similar observations with other preparations indicate the presence of distinct, spatially separated AP-generating loci (nodes) along the VNC and suggest that the initial, stronger stimulus had generated the AP at a node or nodes closer to the recording site. In addition, my experimental results also indicate that functional interconnections occur between the paired medial giant fibers in the abdominal VNC, presumably within each abdominal ganglion. Injection of large (100–200 nA) positive currents into a medial giant fiber submyelinic gap usually triggered an AP, as originally observed by Kusano (1966) in *P. japonicus*. AP triggering presumably occurred when the current density at a neighboring functional node surpassed threshold values. The records in Fig. 4C,D, from two different preparations, provide additional information. In each preparation, following the injection of positive current (bottom trace) into the right medial giant through a separate electrode, an initial and then a secondary AP was

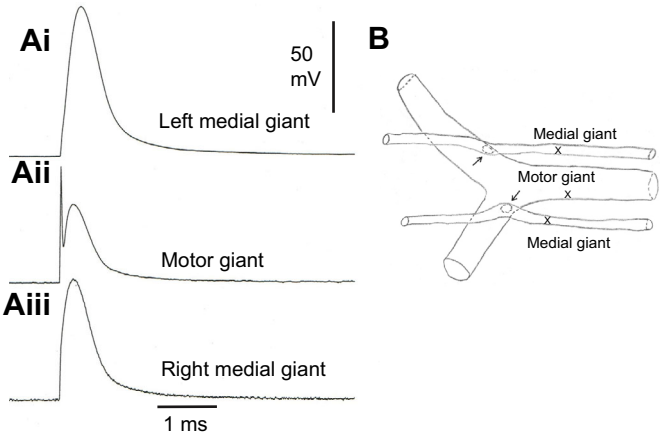

Fig. 3. Temporal relationships of APs in the medial and motor giant fibers. (A) Simultaneous electrical recordings in the second abdominal segment from the left medial giant fiber (Ai), the motor giant fiber (Aii) and the right medial giant fiber (Aiii) following a suprathreshold electrical stimulus to the VNC rostral to the first abdominal ganglion. All recordings were from the submyelinic gap. Note that the peak of the AP in the left medial giant fiber occurs after the motor giant AP peak, a possible consequence of the excitation in the left medial giant fiber having occurred at a more distant functional node, hence with a longer latency, than excitation in the right medial giant fiber. (B) Approximate recording locations (crosses); rostral is to the right. Arrows indicate the presumed location of synapses between the medial giant fibers and the two branches of the motor giant fiber.

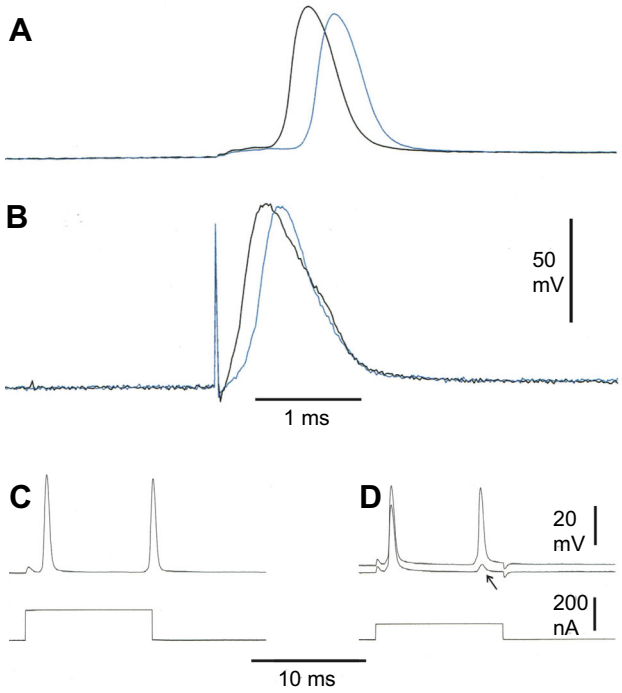

Fig. 4. Latency changes in medial giant fiber APs with changes in stimulus strength. (A,B) Superimposed electrical records of evoked APs in the left (A) and right (B) medial giant fibers in response to strong (black traces) and weaker (blue traces) electrical stimulation of the caudal VNC. Stepwise changes in latency are believed to be due to AP generation at nodes that are closer (black traces) or farther (blue traces) from the recording site. (C,D) Electrical records (upper traces) from medial giant fibers in two different preparations in response to large, positive currents (lower traces) injected into the opposite medial giant fiber. In both cases, an AP generated in the current-injected medial giant fiber evoked an initial and a delayed AP in the opposite fiber, logically through functional connections between the medial giant fibers within a neighboring ganglion. In D, a subsequent current pulse (lower trace) identical to the first (upper trace) generated an initial AP followed by just a collateral potential (arrow), presumably electrotonically derived from a point of functional connectivity.

Journal of Experimental Biology (2017) 220, 3771-3781 doi:10.1242/jeb.166413

observed in the left medial giant fiber, responses that could only have arisen via functional connections between the two medial giants within the abdominal VNC. These and similar observations in other preparations indicate the presence of either synaptic or collateral interconnections between the medial giant fibers at one or more locations within the abdominal nerve cord of *F. duorarum*.

Response of the medial giant fibers and the motor giant fiber to current injections

When two microelectrodes were inserted close to one another in the submyelinic gap of a medial giant fiber, electrotonic potentials were generated in response to injected current of both polarities. Fig. 5 shows examples of the responses to current injection into a medial giant fiber and the motor giant fiber in the same segment. Positive or negative currents injected into the medial giant submyelinic gap generated essentially linear potential changes (Fig. 5A) in the gap with respect to ground over the range tested, with the largest positive currents triggering APs that were transmitted across the medial motor giant synaptic nexus but which did not directly pass in either direction through the synapse (Fig. 5B). Conversely, in other preparations, currents injected directly into the motor giant submyelinic gap or even into the axon itself generated potential changes in the gap or axon but also did not pass across the synaptic nexus. Experiments with other preparations produced similar results, as shown, for example, in Fig. 6. In no instance of observations with more than a dozen preparations were injected currents of either polarity or in either direction observed to modify the postsynaptic potential. The observations presented in Fig. 6 are graphed quantitatively in Fig. 7. A consistent observation of the response to current injections into either the medial giant fibers or the motor giant fibers, exemplified by the graphs presented in Figs 7 and 8, was the complete absence of voltage sag to depolarizing currents usually observed in other neurons, and due to the delayed rectification produced by voltage-gated potassium channels. While the myelin sheath would not be expected to exhibit any non-linear response to current injection, it is clear that a significant proportion of the depolarizing current injected into the submyelinic gap crosses the axonal membrane, as it generates APs at a neighboring node and it would be expected to affect conductance changes in any voltage-sensitive potassium channels that might be present. In a few preparations, only with the largest depolarizing currents was there a possible hint that the slope of the current–voltage (*I*/*V*) curve was becoming more shallow with increasing current.

The failure to observe direct passage of current across the synapse is puzzling. Transmission across the medial giant/motor giant synapse in the shrimp is at least as fast (50–100 µs) as that observed at the medial giant–motor giant nexus in crayfish (Furshpan and Potter, 1959), and it therefore is presumably electrical. Additionally, electron microscopic studies of the analogous medial-to-motor giant synapse in *P. japonicus* suggested the presence of gap junctions between the plasma membranes of the two axons, although presynaptic vesicles and postsynaptic densities were also present in some preparations (Kusano and LaVail, 1971).

In isolated nerve cord preparations, in which the minor and major branches of the motor giant axons were transected near the VNC, even injected currents as large as 200 nA were insufficient to change the electrical potential of the motor giant axon by more than a few millivolts. The very low ‘input resistance’ of the motor axon or the gap (e.g. Fig. 7B) could be due to short circuiting of the gap’s electrical integrity caused by the severed branches, and this appeared to be at least partly the case. Accordingly, some experimental procedures were performed on far less-reduced preparations, where the motor giant branches into the abdominal flexor muscles remained completely intact. In these preparations, the VNC was exposed by a ventral approach, left *in situ* within the abdomen, and access to the motor giant and medial giant fibers was obtained by removing the connective tissue sheath around the VNC in one abdominal segment, gently separating the two connectives at the midline, and dissecting away most of the non-giant axons ventral to the fused motor giant axons. With proper lighting, the fused motor giant fiber usually could be visualized just ventral to the more dorsally and laterally positioned medial giants. As with isolated nerve cord preparations, this approach allowed current-injecting and voltage-recording microelectrodes to be positioned in both sets of giant fibers, and *I*/*V* relationships in the motor giant were obtained that were somewhat closer to the range of those in the medial giant fibers, shown in Fig. 8A. However, there was still no evidence for direct passage of injected current across the synaptic connection, in either direction, whether the current was injected into the motor giant axon or the submyelinic space in the medial giant axons.

As a final test of my procedures in attempting to pass injected current directly across the medial-to-motor giant synaptic nexus, in a few preparations current was passed directly into one of the medial giant fibers and the voltage response was recorded in that fiber, the paired medial giant, and the motor giant, all in the same interganglionic segment. Typical results are shown in Fig. 8B. The voltage response to even the highest injected currents (200 nA) is flat for both the opposite medial giant and the motor giant fiber, indicating that little, if indeed any, DC current was being transferred.

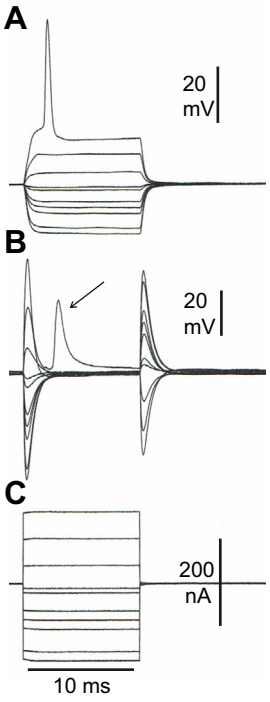

Fig. 5. Current/voltage (*I*/*V*) relationships in medial giant fibers. (A) Voltage responses of a medial giant fiber to currents injected into its submyelinic space (C). Very large positive currents were usually required to evoke an AP. (B) Simultaneously recorded responses of the motor giant fiber to the same currents. No direct transfer of currents across the synapse occurred, although the AP evoked in the medial giant fiber by the largest positive current did generate a postsynaptic spike (arrow) in the motor giant fiber. Large capacitative artifacts occur at the onset and cessation of the current pulses.

Journal of Experimental Biology (2017) 220, 3771-3781 doi:10.1242/jeb.166413

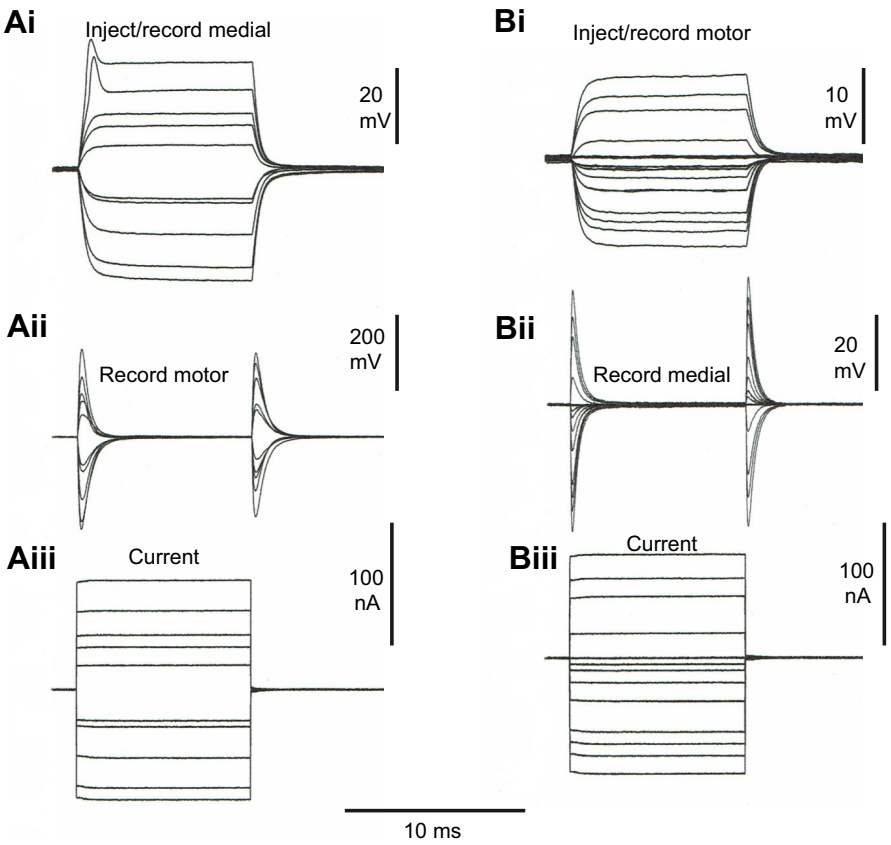

Fig. 6. *I*/*V* relationships in medial and motor giant fibers. (Ai,Bi) Voltage responses of a medial giant fiber (Ai) and the ipsi-segmental motor giant fiber (Bi) to direct injection of positive and negative current pulses (Aiii,Biii). In Ai, the two largest positive pulses each generated a spike shortly after current onset. No spikes were generated in the motor giant fiber by similar currents, possibly because of a low input resistance. (Aii,Bii) Voltage responses in the ipsi-segmental motor giant (Aii) and medial giant (Bii) fiber to the injected currents. No steady trans-synaptic current passage of either polarity occurred.

DISCUSSION

My observations with *F. duorarum* confirm the findings of Kusano (1966), Kusano and Lavail (1971) and Hsu and Terakawa (1999) regarding AP propagation and recording in the myelinated medial giant interneurons of related penaeid shrimps. Conduction velocity in the medial giant fibers is very rapid and APs of nearly 100 mV can be recorded from the gap between the myelin sheath and the axon itself, presumably as a result of the high electrical resistance of the myelin sheath and the relatively low resistivity of the gap fluid compartment (Hsu and Terakawa, 1999). The current studies, furthermore, provide new evidence that, in *F. duorarum*, the medial giant axons are functionally interconnected within the abdominal VNC, presumably within the ganglia themselves. This arrangement would insure symmetrical activation of the abdominal flexor muscles during an escape reaction, and is similar to the interconnections between the abdominal lateral giant fibers in crayfish described anatomically by Johnson (1924), and observed and termed ‘collateral synapses’ by Furshpan and Potter (1959) in their electrophysiological study. Presumably, such interconnections would be bidirectional. APs evoked in one giant axon are transmitted through collateral synapses in adjacent ganglia to the opposite giant axon, where they can propagate in either direction, including back to a ganglion near the original site of stimulation. In the records published by Furshpan and Potter (1959, their fig. 5) such circular excitations occurred for at least four cycles. Similar segmental functional interconnections, via small collateral axons, occur between the paired giant axons of the marine polychaete worm *Sabella penicillus* (Mellon et al., 1980).

Intracellular staining of the motor giant axons with biocytin/neurobiotin mixture and backfilling with cobalt chloride confirmed, as first reported by Faulkes (2015), that the separate myelinated motor giant axons in the third roots are fused together as a single neurite, also myelinated, within the VNC. In each abdominal segment, the fused neurite courses rostrally, is reduced in diameter and, within the parent ganglion, bifurcates to paired clusters of 30–40 small cell bodies. This anatomical situation is different from that in crayfish, where each motor giant axon in the abdominal VNC is separate from its contralateral partner and arises from a single soma. In the caridean prawn, *Palaemonetes vulgaris*, the motor giant axons are also fused between an abdominal ganglion and its third roots, but the two axons arise from just a single pair of cell bodies (Johnson, 1924).

Curiously, whereas neurobiotin can migrate across the gap junctions at rectifying electrical synapses between the lateral giant axons and afferent interneurons in the crayfish *Procambarus clarkii* (Antonsen and Edwards, 2003), this did not occur in *F. duorarum*; the medial giant axons were never stained following injection of the biocytin/neurobiotin mixture, or cobalt, into the motor giant fibers, even though electron micrographic evidence suggests that they are connected by gap junctions (Kusano and LaVail, 1971). This negative finding has a bearing on the interpretation of physiological observations discussed below. Electrical activity in the medial giant axons is rapidly transferred to the motor giant axons via a synaptic connection near their exit from the VNC in the third roots. While precise measurements of synaptic delay were not made, simultaneous recordings in several preparations suggest that it is shorter than 90 µs at 17.5°C. This most assuredly rules out conventional chemical synaptic action.

An unusual observation following the injection of direct current into either the medial or the motor giant fibers was the absence of apparent delayed rectification in the voltage response, exemplified by *I*/*V* curves with linear slopes. This implies that the axonal membranes lack voltage-sensitive potassium channels at the functional nodes. In fact, the voltage-clamp studies of the

Journal of Experimental Biology (2017) 220, 3771-3781 doi:10.1242/jeb.166413

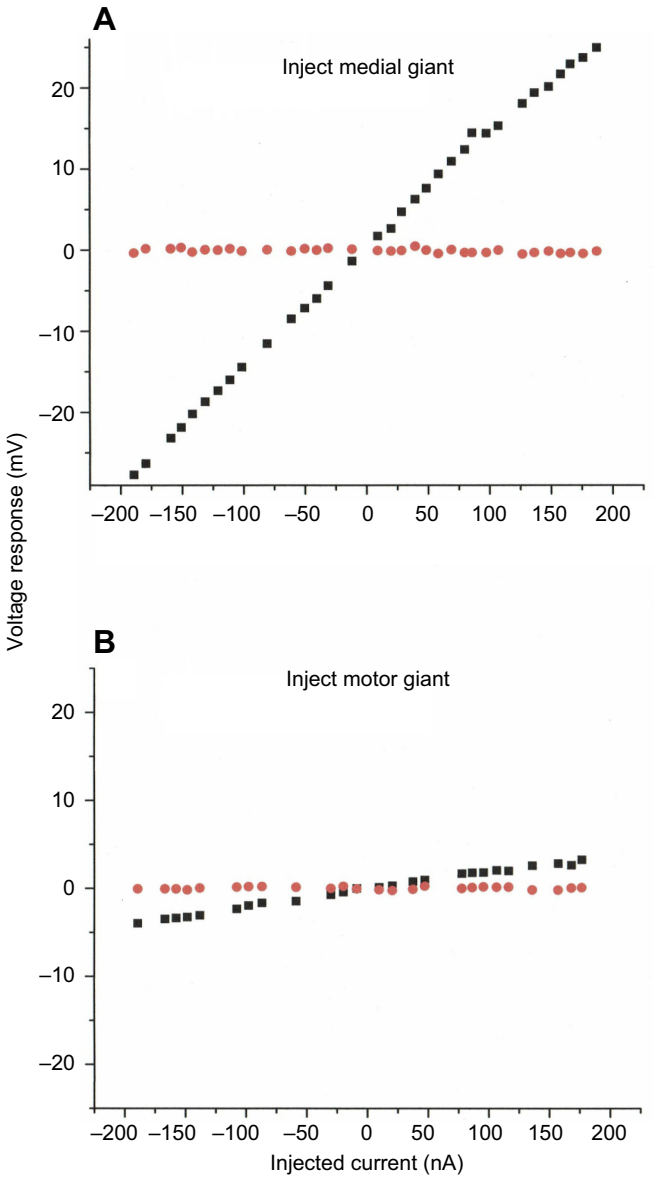

Fig. 7. Graphs of injected current and response in medial and motor giant fibers in an isolated VNC. (A) *I*/*V* relationship (black squares) recorded in a medial giant fiber submyelinic gap in response to current injections using an adjacent microelectrode. The curve is best fitted by a straight line with a slope of 0.127 MΩ (R^2=0.99). The response of the motor giant axon to the same currents (red circles) is flat. (B) *I*/*V* relationship (black squares) in the same motor giant axon to injected current from an adjacent microelectrode. The curve is best fitted by a straight line with a slope of 0.019 MΩ (R^2=0.99). The corresponding curve for the voltage response of the medial giant fiber to the same currents (red circles) is flat.

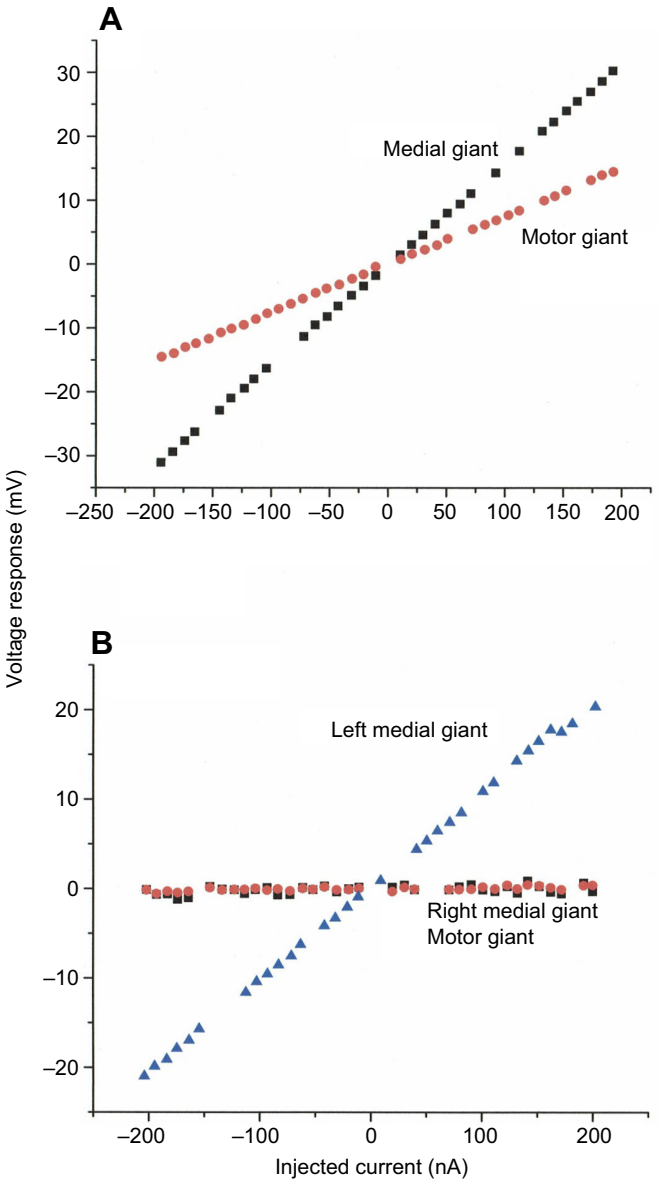

Fig. 8. Graphs of injected current and response in a minimally reduced preparation. (A) *I*/*V* relationship of the medial giant fiber (black squares) and the motor giant axon (red circles) in the same abdominal segment in a minimally reduced preparation (see text on p. 6, bottom of right-hand column). The medial giant curve is best fitted by a straight line having a slope of 0.157 MΩ (R^2=0.99). The motor giant curve is fitted best by a straight line with a slope of 0.075 MΩ (R^2=0.99). (B) *I*/*V* relationship of a medial giant fiber (blue triangles) to a series of injected currents. The curve is best fitted by a straight line with a slope of 0.103 MΩ (R^2=0.99). The flat curves represent simultaneously recorded voltage responses to the same current series of the opposite medial giant (red circles) and the motor giant (black squares) fibers.

fenestration nodes in the medial giant fibers of the shrimp *P. japonicas* (Terakawa and Hsu, 1991) revealed a robust presence of voltage-gated sodium ion channels but little evidence for a comparable density of voltage-gated potassium ion channels, the presence of which was revealed only with depolarizing voltage steps greater than 50 mV. These experimental findings suggest a physiological basis for my own observations.

The difficulty encountered in attempting to pass direct current across the medial-to-motor synaptic connection is not easily explained on the basis of electrical synapses in other crustacean systems. In the crayfish lateral-to-motor giant synapse, current passage is voltage dependent, and the trans-synaptic potential change, V_s, will be positive so long as $V_s=V_{pre}-V_{post}$ (Furshpan and Potter, 1959). The synapse is therefore rectifying, in that if the postsynaptic membrane is depolarized with respect to the presynaptic membrane, little current can pass across it. Elsewhere in the neural circuitry of crayfish escape behavior, the mechano-receptive afferent inputs to the lateral giant fibers also occur via rectifying electrical synaptic connections (Edwards et al., 1991, 1998), the afferent terminals are interconnected via non-rectifying electric synaptic junctions (Herberholz et al., 2002; Antonsen and Edwards, 2003),

Journal of Experimental Biology (2017) 220, 3771-3781 doi:10.1242/jeb.166413

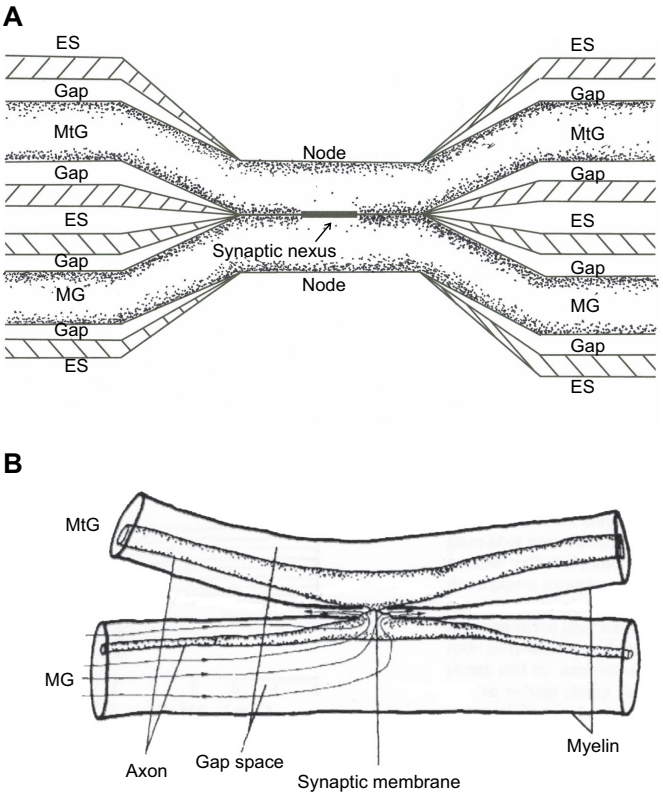

Fig. 9. Anatomical relationships in the medial-to-motor giant synapse. (A) An interpretation of possible anatomical relationships at the medial-to-motor giant synaptic nexus. The medial and motor giant axons are stippled to delineate them from the submyelinic gap. The synaptic locus is assumed to be in proximity to the point where the median giant fiber and motor giant fiber cross one another near the exit of the third roots from the VNC. Cross-hatching represents myelin. ES, extracellular space; Gap, submyelinic gap; MtG, motor giant axon; MG, medial giant axon. Dark bar represents the putative synaptic nexus. (B) Drawing of the medial giant–motor giant synaptic connection at the motor giant exit rostral to the first abdominal ganglion in *Penaeus japonicas*. In this rendition, nodal current in the medial giant fiber exits the axon to extracellular space immediately surrounding the synaptic connection (modified from Terakawa and Hsu, 1991, with permission).

and the segmental giant fibers are rectifying in opposite directions at their input and output terminals (Heitler et al., 1991). The lateral giant fibers in crayfish are actually segmented axons making end-to-end septal, non-rectifying electrical junctions with one another (Kao, 1960). All of these electrical contacts will pass DC current in the appropriate direction across the synaptic nexus.

Fig. 9A is an anatomical schematic diagram of the synapse between the penaeid medial giant axon and the motor giant axon, based upon the descriptions in Kusano and LaVail (1971) and Terakawa and Hsu (1991). Fig. 9B is a more anatomically precise illustration of the synapse, adapted from Terakawa and Hsu (1991); it suggests that the synaptic contact is surrounded on the presynaptic side by a medial giant functional node having a possible membrane area of 500 μm^2. If the shrimp medial-to-motor giant synapse operates through a different electrical mechanism from the rectifying junctions found in crayfish, as my data indicate, it might be one based upon capacitance, as suggested by the electrical schema in Fig. 10. Briefly, the proposed connection consists of two capacitors in series: the apposed plasma membranes of the medial and motor giant axons. Terakawa and Hsu (1991) found that the nodal sodium channel activation rise time, at 100 µs, was faster than in any other system studied to date. They suggest, furthermore, that the sodium channel density at the node may be so large as to generate inward current densities as high as 500 mA cm^{-2}. In the micrograph of a fenestration node shown by Terakawa and Hsu (1991) having a radius of 12.5 µm, nearly 2500 nA of current could possibly be available to discharge the membrane capacitance at the point of contact. While the area of the synaptic contact is unknown, Kusano and LaVail (1971) in their electron microscopical study, indicated that: 'The giant fiber to giant motor fiber synapse was observed to involve the invagination of the axons into the connective tissue separating the two nerve fibers by way of one or more blunt processes…The axons made contact with one another at several points.' They go on to say that at all of these points of contact, close appositions of the two membranes were made that, at high magnification, proved to be gap junctions, and where the width of the extracellular space was no more than 2–3 nm (Kusano and LaVail, 1971). While a strictly capacitative excitatory process between the medial giant axons and the motor giant axons is highly speculative at this point, studies by previous authors, as discussed above, suggest that the area of contact is immediately surrounded by a functional node where the transmembrane current density is extraordinarily high and the kinetics are fast. A strictly capacitative mechanism of transmission, if present, would explain why it was never possible to pass direct current across the synapse. Furthermore, it would also offer an explanation for why the biocytin/neurobiotin mixture injected into the motor giant axon never diffused across the synaptic nexus.

Ephaptic interactions between neurons – that is, functional interactions in the absence of conventional chemical or electrical synaptic structures – are known from a few experimental studies. Naturally occurring ephaptic inhibition is also known from the Mauthner neurons in teleost fish, where an elaborate anatomical structure provides an electrical environment conducive to a brief hyperpolarization of the target neuron by an approaching, blocked AP in the opposite Mauthner axon collateral (Furshpan and Furukawa, 1962; Korn and Faber, 1975). A connective tissue structure – the axon cap – surrounding the initial emergence of the target axon from the cell body, ensures that local circuit currents ahead of the approaching 'pre-ephaptic' AP will be injected into the target axon, hyperpolarizing it, instead of being dissipated into the extracellular space. Artificial ephapses between two giant axons have, under extreme experimental conditions, been shown to transfer excitation between them (Katz and Schmitt, 1940; Arvanitaki, 1942). In another, more recent study (Ramon and Moore, 1978), two giant axons from a squid were placed in close proximity to one another, and the region of contact was electrically isolated from the surrounding volume conductor with mineral oil, ensuring a dense extracellular current sink when the AP triggered in one of the axons passed the point of contact. Additionally, the calcium ion concentration in the bathing medium was lowered to reduce AP threshold. Under these conditions, when an AP was generated in one axon by electrical shock, as it propagated through the region of contact, its field potential was sufficient to evoke an AP in the second axon. In all of these cases, special experimental arrangements ensured that a large enough field potential gradient was established by the pre-ephaptic AP that was sufficient to excite the post-ephaptic axon above threshold. In the case of the shrimp medial-to-motor giant synapse, however, the structural and functional details of the immediate postsynaptic (motor) membrane are not known. If they mirror the situation described (Terakawa and Hsu, 1991) for the presynaptic side of the nexus, however, it is reasonable to assume that sufficient charge transfer might occur in the region of membrane apposition, possibly through an ephaptic

Journal of Experimental Biology (2017) 220, 3771-3781 doi:10.1242/jeb.166413

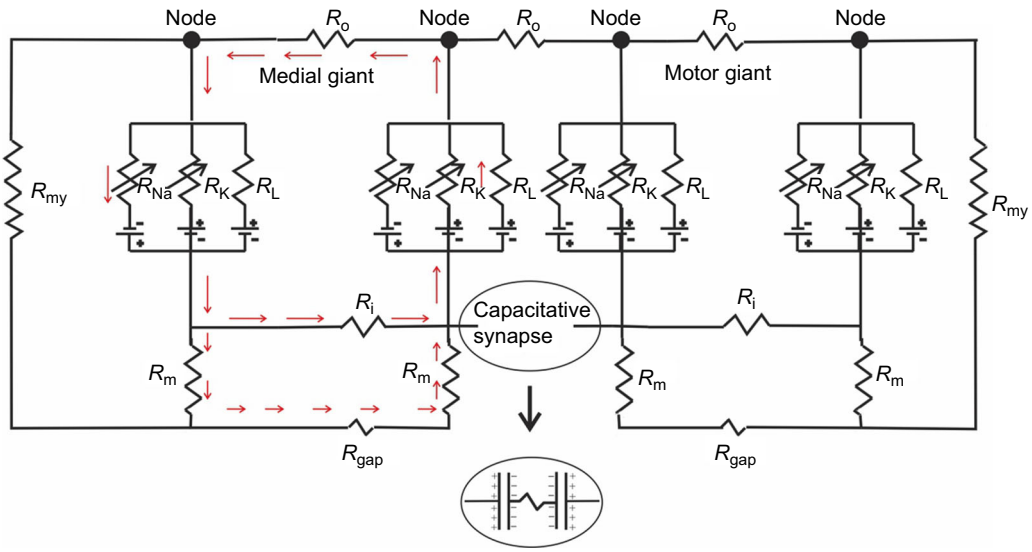

Fig. 10. Electrical analog of the medial-to-motor giant synapse. Diagram of the proposed equivalent electrical circuit in the vicinity of the medial-to-motor giant synaptic nexus. Functional nodes are assumed to flank the synapse on both the presynaptic and postsynaptic fibers. Red arrows indicate current flow during an AP at a medial giant node. While the diagram attributes standard Hodgkin and Huxley conductances to the nodal membrane, voltage clamp studies with the medial giant nodes in *P. japonicas* suggest that the potassium conductance, ΔG_K, may be minimal or non-existent (Terakawa and Hsu, 1991). Inset indicates charge distribution across in-series capacitances at the nexus near the peak of the medial giant AP. R_m, specific resistance of the axonal membrane; R_{my}, specific resistance of the myelin sheath; R_i, axonal resistivity; R_{gap}, submyelinic gap resistivity; R_o, resistivity of the extracellular space; R_{Na}, sodium ion conductance; R_K, potassium ion conductance; R_L, leak conductance. Membrane/myelin capacitances other than at the putative synapse have been omitted for clarity.

mechanism relying on physical principles similar to those in the above citations. If the anatomical considerations of Terakawa and Hsu (1991) are correct, the relatively large area of the surrounding node compared with that of the synaptic contact would be expected to generate large capacitative currents. In theory, there is no disqualifying reason why an ephaptic mechanism based upon very rapid capacitative discharge could not be the basis for excitation transfer between the medial giant fibers and the motor giant fibers in the abdominal segments of the shrimp.

Going forward, serial transmission electron microscopy of the region of connection between the medial and motor giant axons could provide informative data about the anatomical substrates relating to this hypothesis. Furthermore, exposing the synaptic contact to oscillating voltage changes at different fixed frequencies might reveal transfer characteristics that would favor a capacitative mechanism, while performing experimental tests in Ca^{2+}-free saline could definitively rule out a traditional chemical synaptic mechanism.

Acknowledgements

I am grateful to my colleagues Prof. W. Otto Friesen and Prof. Martin Mendelson for reading and commenting on an earlier draft of this paper. The paper has especially benefitted from numberless discussions with Prof. Friesen about the theoretical aspects of synaptic transmission; however, the conclusions are my own.

Competing interests

The author declares no competing or financial interests.

Funding

This research received no specific grant from any funding agency in the public, commercial or not-for-profit sectors.

References

Antonsen, B. L. and Edwards, D. H. (2003). Differential dye coupling reveals lateral giant escape circuit in crayfish. *J. Comp. Neurol.* **466**, 1-13.

Arvanitaki, A. (1942). Effects evoked in an axon by the activity of a contiguous one. *J. Neurophysiol.* **5**, 89-108.

Edwards, D. H., Heitler, W. J., Liese, E. M. and Fricke, R. A. (1991). Postsynaptic modulation of rectifying electrical synaptic inputs to the LG escape command neuron in crayfish. *J. Neurosci.* **11**, 2117-2129.

Edwards, D. H., Yeh, S. R. and Krasne, F. B. (1998). Neuronal coincidence detection by voltage-sensitive electrical synapses. *Proc. Nat. Acad. Sci. USA* **95**, 7145-7150.

Fan, S. F., Hsu, K., Chen, F. S. and Ho, B. (1961). On the high conduction velocity of the giant nerve fiber of the shrimp, *Penaeus orientalis*. *Kexue Tongbao* **12**, 51-52.

Faulkes, Z. (2015). Motor neurons in the escape response circuit of white shrimp (*Litopenaeus setiferrus*). *PeerJ* **3**, e1112.

Furshpan, E. J. and Furukawa, T. (1962). Intracellular and extracellular responses of the several regions of the Mauthner cell of the goldfish. *J. Neurophysiol.* **25**, 732-771.

Furshpan, E. J. and Potter, D. D. (1959). Transmission at the giant motor synapses of the crayfish. *J. Physiol.* **145**, 289-325.

Herberholz, J., Antonsen, B. L. and Edwards, D. H. (2002). A lateral excitatory network in the escape circuit of crayfish. *J. Neurosci.* **22**, 9078-9085.

Heitler, W.J., Fraser, K. and Edwards, D. H. (1991). Different types of rectification at electrical synapses made by a single crayfish neurone investigated experimentally and by computer simulation. *J. Comp. Physiol. A* **169**, 707-718.

Holmes, W. (1942). The giant myelinated nerve fibers of the prawn. *Proc. Roy. Soc. B Lond.* **231**, 293-314.

Hsu, K. and Terakawa, S. (1996). Fenestration in the myelin sheath of nerve fibers of the shrimp: a novel node of excitation for saltatory conduction. *J. Neurobiol.* **30**, 387-409.

Hsu, K. and Terakawa, S. (1999). Fenestration nodes and the wide submyelinic space form the basis for the unusually fast impulse conduction of shrimp myelinated axons. *J. Exp. Biol.* **202**, 1979-1989.

Johnson, G. E. (1924). Giant nerve fibers in crustaceans with special reference to *Cambarus* and *Palaemonetes*. *J. Comp. Neurol.* **36**, 323-373.

Kao, C. Y. (1960). Postsynaptic electrogenesis in septate giant axons. II. Comparison of medial and lateral giant axons of crayfish. *J. Neurophysiol.* **23**, 618-635.

Katz, B. and Schmitt, O. H. (1940). Electric interaction between two adjacent nerve fibres. *J. Physiol.* **97**, 471-488.

Korn, H. and Faber, D. S. (1975). An electrically mediated inhibition in goldfish medulla. *J. Neurophysiol.* **38**, 452-471.

Krasne, F. B. and Wine, J. J. (1975). Extrinsic modulation of crayfish escape behavior. *J. Exp. Biol.* **63**, 433-450.

Kusano, K. (1966). Electrical activity and structural correlates of giant nerve fibers in Kuruma shrimp. *J. Cell. Physiol.* **68**, 361-384.

Kusano, K. and LaVail, M. M. (1971). Impulse conduction in the shrimp medullated giant fiber with special reference to the structure of functionally excitable areas. *J. Comp. Neurol.* **142**, 481-494.

Liu, Y.-C. and Herberholz, J. (2010). Sensory activation and receptive field organization of the lateral giant escape neurons in crayfish. *J. Neurophysiol.* **104**, 675-684.

Mellon, D. F. and Christensen-Lagay, K. (2008). A mechanism for neuronal coincidence revealed in the crayfish antennule. *Proc. Nat. Acad. Sci. USA* **105**, 14626-14631.
Mellon, D. F., Treherne, J. E., Lane, N. J., Harrison, J. B. and Langley, C. K. (1980). Electrical interactions between the giant axons of a polychaete worm (*Sabella penicillus* L.). *J. Exp. Biol.* **84**, 119-136.
Ramon, F. and Moore, J. W. (1978). Ephaptic transmission in squid giant axons. *Am. J. Physiol.: Cell Physiol.* **3**, C162-C169.
Robertson, J. D. (1955). Recent observations on the ultrastructure of the crayfish median-to-motor giant synapse. *Exp. Cell. Res.* **8**, 226-229.
Terakawa, S. and Hsu, K. (1991). Ionic currents of the nodal membrane underlying the fastest saltatory conduction in myelinated giant nerve fibers of the shrimp *Penaeus japonicas*. *J. Neurobiol* **22**, 342-352.
Wine, J. J. and Krasne, F. B. (1982). The cellular organization of crayfish escape behavior. In *The Biology of Crustacea: Vol. 4, Neural Integration and Behavior* (ed. D.C. Sandeman and H. L. Atwood), pp. 241-319. New York: Academic Press.